

RESEARCH ARTICLE

Chemical mutagenesis of *Listeria monocytogenes* for increased tolerance to benzalkonium chloride shows independent genetic underpinnings and off-target antibiotic resistance

Tyler D. Bechtel¹✉, Julia Hershelman^{1,2}✉, Mrinalini Ghoshal^{1,2}, Lynne McLandsborough², John G. Gibbons^{1,3,4*}

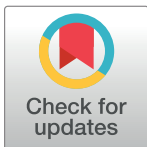
1 Department of Food Science, University of Massachusetts, Amherst, MA, United States of America,

2 Department of Microbiology, University of Massachusetts, Amherst, MA, United States of America,

3 Molecular and Cellular Biology Graduate Program, University of Massachusetts, Amherst, MA, United States of America, **4** Organismic & Evolutionary Biology Graduate Program, University of Massachusetts, Amherst, MA, United States of America

✉ These authors contributed equally to this work.

* jggibbons@umass.edu



OPEN ACCESS

Citation: Bechtel TD, Hershelman J, Ghoshal M, McLandsborough L, Gibbons JG (2024) Chemical mutagenesis of *Listeria monocytogenes* for increased tolerance to benzalkonium chloride shows independent genetic underpinnings and off-target antibiotic resistance. PLoS ONE 19(7): e0305663. <https://doi.org/10.1371/journal.pone.0305663>

Editor: Do-Won Jeong, Dongduk Women's University, REPUBLIC OF KOREA

Received: December 20, 2023

Accepted: June 2, 2024

Published: July 19, 2024

Copyright: © 2024 Bechtel et al. This is an open access article distributed under the terms of the [Creative Commons Attribution License](https://creativecommons.org/licenses/by/4.0/), which permits unrestricted use, distribution, and reproduction in any medium, provided the original author and source are credited.

Data Availability Statement: *L. monocytogenes* FSL-N1-304 whole-genome Illumina and Oxford Nanopore Technologies sequencing data are available through the NCBI SRA run accession numbers SRR17006605 and SRR17067427, respectively. The FSL-N1-304 reference genome assembly is available through GenBank accession number GCA_021391455.1. Illumina whole-genome sequencing data for mut-1 and mut-2 are available through NCBI SRA run accession

Abstract

Listeria monocytogenes, a potentially fatal foodborne pathogen commonly found in food processing facilities, creates a significant economic burden that totals more than \$2 billion annually in the United States due to outbreaks. Quaternary ammonium compounds (QACs), including benzalkonium chloride (BAC), are among the most widely used sanitizers to inhibit the growth and spread of *L. monocytogenes* from food processing facilities. However, resistance to QACs has been increasing in *L. monocytogenes* and different genetic mechanisms conferring resistance have been discovered. Here, we used ethyl methanesulfonate (EMS) to chemically mutagenize the BAC-susceptible strain, *L. monocytogenes* FSL-N1-304. We isolated two mutants with increased tolerance to BAC compared to the parental strain. Next, we assessed the off-target effect of increased tolerance to BAC by measuring the minimum inhibitory concentrations (MICs) of a diverse set of antibiotics, revealing that *mut-1* and *mut-2* displayed significantly increased resistance to fluoroquinolone antibiotics compared to the parental strain. A hemolysis assay was then used to investigate a potential correlation between BAC tolerance and virulence. Interestingly, *mut-1* and *mut-2* both exhibited significantly higher hemolysis percentage than the parental strain. We then sequenced the genomes of the parental strain and both mutants to identify mutations that may be involved in the increased resistance to BAC. We identified 3 and 29 mutations in *mut-1* and *mut-2*, respectively. *mut-1* contained nonsynonymous mutations in *dagK* (a diacylglycerol kinase), *lmo2768* (a permease-encoding gene), and *lmo0186* (resuscitation promoting factor). *mut-2* contained a nonsense mutation in the nucleotide excision repair enzyme UvrABC system protein B encoding gene, *uvrB*, which likely accounts for the higher number of mutations observed. Transcriptome analysis in the presence of BAC revealed that genes related to the phosphotransferase system and internalins were up-regulated in both mutants, suggesting

numbers SRR21641536 and SRR21641535, respectively. Data Availability Statement All files associated with genomic and transcriptomic data in this study can be found under NCBI BioProject PRJNA782601. All other data are available in the manuscript and/or supporting information files.

Funding: This material is based upon work supported by the National Institute of Food and Agriculture, U.S. Department of Agriculture, the Center for Agriculture, Food and the Environment, and the Food Science department at University of Massachusetts Amherst, under project number MAS-00529 to JGG and LM. The sponsor played no role in the study design, data collection and analysis, decision to publish, or preparation of the manuscript.

Competing interests: The authors have declared that no competing interests exist.

their significance in the BAC stress response. These two mutants provide insights into alternative mechanisms for increased BAC tolerance and could further our understanding of how *L. monocytogenes* persists in the food processing environment.

Introduction

Listeria monocytogenes is a gram-positive, foodborne bacterial pathogen that causes a serious infection called listeriosis [1]. Listeriosis is a relatively rare disease, but it can lead to severe and potentially fatal symptoms for elderly and immunocompromised individuals including infections resulting in meningitis and septicemia [2,3]. Additionally, pregnant women are more susceptible to listeriosis, which is particularly problematic as *L. monocytogenes* possesses the unique ability to permeate the placenta and infect the fetus, which can lead to fetal meningitis and miscarriages [4]. A study analyzing data from 2000–2008 revealed that *L. monocytogenes* had the highest hospitalization rate (94%) and third highest fatality rate (15.9%) among 31 major foodborne pathogens [5].

L. monocytogenes is highly abundant in the natural environment and capable of surviving adverse conditions, resulting in frequent contamination and persistence of *L. monocytogenes* strains in food processing facilities [6]. Given the health concerns and economic impacts of *L. monocytogenes* contamination in the food industry, the FDA has established guidelines to prevent contamination and outbreaks in foods [7]. These guidelines include personal protective equipment for workers, structured operation plans of the plant, specific equipment, testing protocols, and sanitization [8].

Quaternary ammonium compounds (QACs) are a class of antimicrobial compounds commonly used for surface sanitization in food processing facilities [9]. The bactericidal mode of action for QACs is similar to that of a detergent [10]. The negatively charged bacterial cellular membrane interacts with the positively charged head of the QAC molecule, allowing the non-polar QAC side chains to disrupt the intramembrane region. This interaction leads to the formation of micelles, cytosolic leakage, and eventual cellular lysis [11]. Benzalkonium chloride (BAC) is a type of QAC that is a common component of commercial disinfectants that are used to sanitize solid surfaces in food processing facilities [9,12]. Over the last two decades, several studies have reported increased BAC tolerance in *L. monocytogenes* strains isolated from food environments [13–18]. An increase in QAC tolerance has been attributed to improper application, dilution, and biodegradation of QACs resulting in sub-lethal concentration gradients [19,20]. Several mechanisms for BAC resistance have been discovered. Most commonly, BAC resistance, or increased tolerance, involves alterations to efflux pumps [14,16,21–23]. Adaptation to BAC can also result in cross-tolerance to fluoroquinolone antibiotics, suggesting shared resistance mechanisms [24–27]. Thus, the improper usage of BAC, and subsequent adaptation, could be contributing to off-target antibiotic resistance [24,28].

The goal of this study was to investigate the potential genetic mechanisms and transcriptome response underlying adaptation to BAC and the effects of BAC adaptation on antibiotic resistance. We used chemical mutagenesis combined with whole-genome sequencing (Mut-seq) to isolate mutants with increased tolerance to BAC and to identify candidate mutations. Additionally, we analyzed the transcriptome of BAC tolerant mutants and the parental strain during exposure to BAC to identify genes and pathways responsive to BAC exposure. We also measured the hemolytic activity of the WT and mutant strains to investigate potential a relationship between BAC tolerance and virulence. Finally, we measured the minimum inhibitory concentration of several antibiotics in the wild-type and mutants to determine if increased tolerance to BAC resulted in changes in antibiotic sensitivity.

Methods

Bacterial isolates and culture conditions

Isolate FSL-N1-304 was selected at random from our collection of benzalkonium chloride resistant isolates, as we were screening for gain of function phenotypes. FSL-N1-304 was obtained from the *L. monocytogenes* strain collection at Cornell University's Food Safety Laboratory. This strain was originally isolated from floor drains in a fish processing facility in New York, USA [29]. All strains were cultured at 37°C in tryptic soy broth media supplemented with 0.6% yeast extract (TSB+YE).

Chemical mutagenesis using ethyl methanesulfonate (EMS)

Chemical mutagenesis was performed using a previously described protocol with several alterations [30]. Our complete overall experimental design is depicted in Fig 1. First, 1 ml of cells was harvested from an overnight culture through centrifugation at 2,380 x g for 10 minutes. The cells were then washed twice with 1 ml phosphate buffered saline (PBS). After washing, the pellet was resuspended in 120 mM of EMS suspended in 1 mL of PBS. For a non-mutagenized control, 1 mL of PBS was added to the wild-type (WT) cells. All tubes were incubated for 1 hour at 37°C. Finally, cells were washed three times with PBS to remove EMS and resuspended in 1 mL of PBS.

Determining benzalkonium chloride minimum inhibitory concentration

100 µl of overnight culture of FSL-N1-304 WT cells were inoculated on tryptic soy agar (TSA) +YE agar plates supplemented with 1, 2, 3, 4, and 5 µg/ml benzalkonium chloride (BAC) and

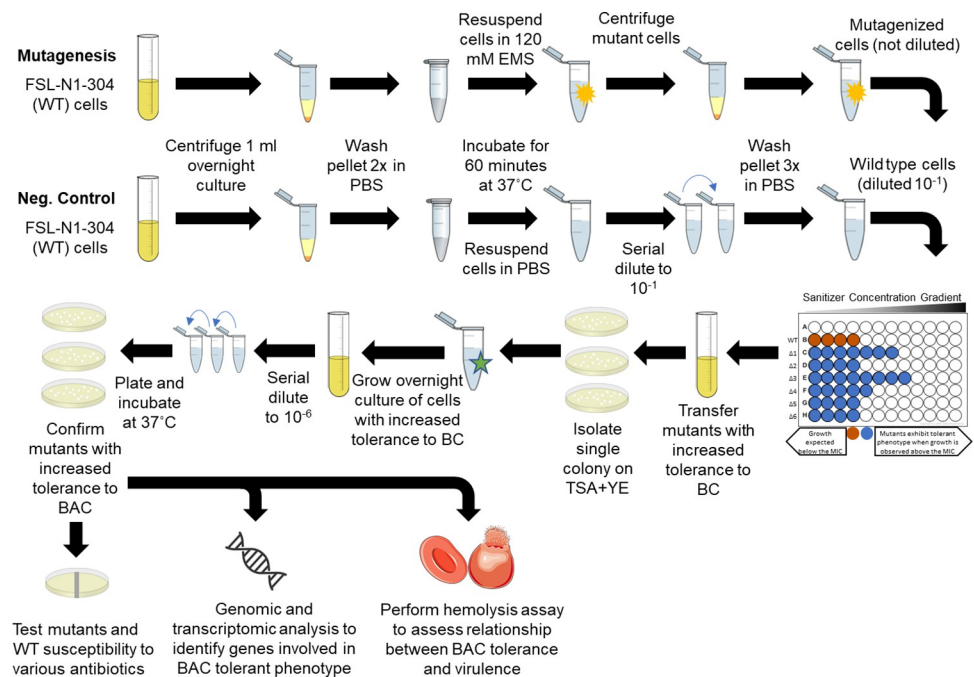


Fig 1. Experimental approach for identifying EMS derived *L. monocytogenes* mutants with increased tolerance to benzalkonium chloride. Experimental approach used for chemical mutagenesis, mutant screening for increased tolerance to benzalkonium chloride, antibiotic susceptibility determination and whole genomic sequencing of mutants with increased tolerance to benzalkonium chloride. Portions of this figure utilized images from [Clicer.com](https://www.clicer.com/), licensed under Creative Commons CC0 1.0, and Servier Medical Art, licensed under Creative Commons Attribution 4.0.

<https://doi.org/10.1371/journal.pone.0305663.g001>

incubated for 48 hours at 37°C to determine the minimum inhibitory concentration (MIC). The MIC was defined as the lowest BAC concentration in which no cell growth was observed. Automated colony quantification and plate imaging was performed using an Interscience Scan1200 (Interscience, Saint-Nom la Bretèche, France).

Next, mutants were screened for increased tolerance to BAC in liquid media by inoculating EMS exposed cells into a 96 well plate (BioLite 96 Well Multidish—Thermo Scientific) with BAC concentrations ranging from 0–11 µg/ml, in increments of 1 µg/ml. The top row in each plate represented a negative control which was prepared by adding 50 µl PBS to each well rather than the inoculum. After plating 100 µl of cells treated with EMS and 100 µl of untreated cells on TSA+YE plates, we found that exposure to EMS resulted in a 1-log reduction in cell viability. After a 24-hour incubation there was 2.35×10^8 CFU/ml of untreated WT cells, and 8.41×10^7 CFU/ml of EMS treated cell. Thus, to normalize the cell density across WT and mutagenized cells, we diluted the WT cells 10-fold to bring the final cell density of the inoculum to approximately 1×10^8 CFU/ml. The remaining rows were inoculated with 50 µl of the mutant cells, undiluted, immediately after exposure to EMS. The 96 well plate was incubated at 37°C for 24 hours, and optical density at 600 nm (OD_{600}) was measured using a BioTek (Winooski, VT, USA) Elx800 microtiter plate reader. Cell density was used to screen the mutants for BAC tolerant phenotypes. We set a threshold for viable cell growth when $OD_{600} \geq 0.1$, as previously described [31].

Validation and MIC determination of increased BAC tolerance in mutants

For mutant cultures that exhibited increased BAC tolerance during screening in 96 well plates, 100 µl was transferred from the wells and inoculated into fresh TSB+YE media and grown overnight. The overnight cultures were then plated on to TSA+YE to isolate single colonies of *mut-1* and *mut-2*. These single colonies were grown overnight in TSB+YE and freezer stocks were prepared in 15% glycerol. All subsequent experimentation was conducted from these stocks.

To validate the BAC tolerant phenotypes observed in the initial screen, overnight cultures of mutants and WT were subjected to the similar BAC screening process as described above using the overnight cultures but in triplicate. After observing that the mutants grew to 6 µg/ml BAC on the 96 well plate during the original screening following mutagenesis, the screening plate was set up similarly, but only included media with 0–7 µg/ml BAC, and this time included three biological replicates for the WT and each mutant. After 24 hours OD_{600} readings were collected using a microtiter plate reader. The MIC was recorded as the concentration of BAC in the first well that had an $OD_{600} < 0.10$.

Frozen stocks of the WT and mutants were also used to screen for the MIC of BAC on solid media. Overnight cultures of the WT and mutants were diluted to approximately 1×10^4 CFU/ml and 100 µl of each diluted culture was spread on tryptic soy agar and yeast extract (TSA+YE) plates, as well as TSA+YE plates supplemented with 0, 1, 2, 3, 4, 5, 6, 7 µg/ml BAC. Plates were incubated at 37°C for 48 hours, then images of the plates were obtained and the colonies were quantified using an Interscience Scan1200. The MIC was recorded as the first plate that had no observable colonies for each strain.

Bacterial growth curve and fitness trade-off analysis

Overnight cultures of WT and mutant cultures were standardized to an OD_{600} of 1.0, and subsequently diluted ten-fold in sterile PBS to achieve a final inoculum of $\sim 10^4$ CFU/ml. A 5 µl volume of this inoculum was then added in triplicate to a 96-well plate (BioLite 96 Well Multidish—Thermo Scientific) with wells each containing 200 µl of TSB+YE (control), TSB+YE+2 µg/

ml BAC, or TSB+YE+3 $\mu\text{g/ml}$ BAC. Cultures were then grown for 48 hours at room temperature and growth kinetics were measured using the oCelloScope (Biosense Solutions, Denmark) with the following parameters: auto-illumination, auto-focus, image distance = 4.9mm, images per repetition = 5, repetitions = 48, and repetition interval = 1 hour. Total absorption measurements were recorded using a fixed 505 nm wavelength and growth kinetic analysis was conducted using the normalized total absorption algorithm.

***hly* virulence assay.** We measured *hly* activity as a proxy for virulence to test if this virulence phenotype was altered in the BAC tolerant mutants compared to the parental strain. *hly* encodes listeriolysin O, which is required for pathogenesis. Hemolytic activity was measured for WT and mutant strains based on a previously described method with minor alterations [32]. Briefly, 1 mL of overnight cultures were centrifuged at 14,000 x g for 10 minutes to pellet the bacteria. The supernatant (crude exosubstance) was then transferred to a new microcentrifuge tube and the pellet was discarded. The crude exosubstance was diluted two-fold in PBS in a 96-well plate (Biolite Microwell Plates; ThermoFisher Scientific), leaving a final volume of 100 μl in each well. Negative control wells (0% hemolysis) were prepared with 100 μl sterile PBS. Complete hemolysis (100%) control wells were prepared with 100 μl PBS + 1% Triton X-100. A sheep blood solution was prepared by washing pooled, defibrinated sheep blood (Carolina Biological, Burlington, NC) in cold PBS by repeated centrifugation at 600 x g for 10 minutes. Washing steps were repeated until the supernatant appeared clear and colorless. The clean red blood cell (RBC) pellet was then diluted in cold PBS + 20mM cysteine to a 3% RBC suspension. 100 μl of the 3% RBC suspension was then added to each well and mixed by pipetting. The microtiter plate was then incubated at 37°C for 30 minutes. Absorbance readings were performed using an Elx800 absorbance reader (BioTek; Winooski, VT, USA). The following formula was used to quantify the hemolysis percentage: $\text{Hemolysis \%} = \left(1 - \frac{\text{OD}_s}{\text{OD}_t}\right) \times 100$, where OD_s is the difference in optical density at 620nm between the sample and the positive control well and OD_t is the difference in optical density at 620nm between the negative and positive control wells.

Determining the minimum inhibitory concentration of antibiotics

Minimum inhibitory concentration test strips (Liofilchem S.r.l.; Roseta, Italy) were used to determine the MICs of ciprofloxacin, gentamicin, erythromycin, ampicillin, tetracycline, norfloxacin, penicillin G, and vancomycin in the WT and mutant strains. Overnight cultures of *L. monocytogenes* WT and mutants were diluted to 10⁹ CFU/ml and spread onto TSA+YE plates using a spreader. Following the manufacturer's instructions, the Liofilchem strip was positioned on the surface of agar using sterile forceps, and plates were incubated at 37°C for 24 h. Plates were then imaged and MICs were recorded for the WT and mutants for each antibiotic. The MIC was determined by observing where the zone of inhibition ellipse intersected the MIC test strip. This assay was performed in duplicate and averaged to determine the final MIC for each antibiotic. MIC values were classified as susceptible, intermediate, or resistant to the antibiotic according to CLSI breakpoint values for *Staphylococcus* spp. [33]. Because antibiotic breakpoints for CLSI, EUCAST or FDA are not reported for *L. monocytogenes*, we chose to report breakpoints for *Staphylococcus* spp as it is the most closely related.

Whole genome sequencing of FSL-N1-304 and BAC tolerant mutants

From a frozen stock, WT cells were inoculated in TSB+YE media and incubated for 24 hours at 37°C. 1 mL of the overnight culture was centrifuged at 14,000 x g for 10 minutes to pellet the cells. DNA extraction was performed on the pelletized cells using the PureLink Microbiome DNA Purification Kit (Invitrogen; Carlsbad, CA) following the manufacturer's instructions.

For the WT strain, 150-bp paired-end libraries were generated at the Microbial Genome Sequencing Center (Pittsburgh, PA, USA) and sequenced on a NextSeq 2000 sequencer (Illumina; San Diego, CA, USA). Low quality reads were trimmed and adapter sequences were removed from Illumina sequences using *bcl2fastq* (version 2.20.0.445) (RRID:SCR_015058) [34]. Oxford Nanopore Technologies (ONT) (Oxford, UK) PCR-free ligation library preparation was also used to generate long sequence reads. ONT reads were adapter and quality trimmed using *porechop33* (version 0.2.3_seqan2.1.1) (RRID:SCR_016967) [35]. Hybrid assemblies were generated from Illumina and ONT reads using *Unicycler* (version 0.4.8) and assembly quality was assessed using *QUAST* (version 5.0.2) [36,37]. Gene models were predicted with functional annotations using *Prokka* (version 1.14.5) with default parameters and ‘*—rfam*’ [38]. Culturing and DNA extraction of mutant strains was performed with the same protocol as the WT and 150-bp paired-end libraries were generated using Illumina sequencing as described above [34,36–38].

Identifying mutations in BAC tolerant mutants

TrimGalore version 0.3.7 (RRID:SCR_011847) was used to trim adapter sequences and trim reads at low quality positions with the following parameters: *—quality 30,—stringency 1,—gzip,—length 50* [39,40]. All subsequent software was used with default parameters unless otherwise specified. *BWA* (version 0.7.15) (RRID:SCR_010910) was used to map the mutant resequencing data against the ancestral reference genome [41]. *Samtools* (version 1.4.1) (RRID:SCR_002105) and *bamaddrg* (<https://github.com/ekg/bamaddrg>) were used to index and add sample names to the sorted BAM files, respectively [42]. Joint genotyping for SNPs and short indels of the mutants was performed using *Freebayes* (version 1.3.1) (RRID:SCR_010761) [43]. *GATK* (v. 4.0.6) was used to convert the resulting VCF files into table format [44]. A *SnEff* database was built for the FSL-N1-304 WT reference genome and SNP annotation prediction was performed in the mutant strains using *SnEff* (version 4.1) [45]. Large-scale Blast Score Ratio (LS-BSR) was used to investigate gene presence/absence mutations using default parameters with the exception of “*-b blastn -c cdhit*” [46]. The InterPro server was used to predict protein domains in candidate proteins (<https://www.ebi.ac.uk/interpro/>) [47].

RNA-sequencing and differential gene expression analysis

We performed RNA-seq on the WT and mutant strains in the presence of BAC in order to compare their transcriptome profiles. Each culture was revived from freezer stocks by growing in TSB+YE overnight at 37C. 100µl of overnight cultures was then passaged into TSB+YE containing 2 µg/ml BAC and grown to mid-log phase (10 hours). This concentration of BAC was chosen because it was the highest we could grow the WT without completely inhibiting growth, allowing us to compare the transcriptome response to BAC stress in both the WT and the mutants. Bacteria were then centrifuged at 14,000 x g for 10 minutes to obtain bacterial pellets which were rapidly frozen using dry ice. RNA extraction, ribosomal depletion library preparation and sequencing were performed at SeqCenter (Pittsburg, PA). Sequencing was performed on a NovaSeq 6000 (Illumina; San Diego, CA, USA), generating 2x51bp reads. Three biological replicates were sequenced for each sample. Adapter trimming and demultiplexing were performed with *bcl-convert* (v4.0.3) [34]. Genome indexing and mapping were performed using *bwa* (v0.7.17) with default parameters [41]. *Samtools* (v1.14) was used to sort and index BAM files [42]. *Bedtools2* (v2.30.0) was used to extract read counts per transcript from gene coordinates in the sorted BAM files [48]. The *DESeq2* (version 1.38.3) package was used in R (version 4.2.3 and RStudio 2023.03.1+446) to normalize read counts and identify differentially expressed genes [49]. Differential expression thresholds were defined using log-fold

change [$\log_2(\text{FC})$] values >1 (up-regulated) and <-1 (down-regulated). A p-value significance threshold was also defined using the multiple test corrected p-value $1.6\text{E-}5$. Principal component analysis (PCA) was performed on DESeq2 normalized read counts using JMP Pro (version 17) to examine the relationship between samples and replicates [50]. Volcano plots of gene expression (DESeq2 normalized read counts) and p-value were generated using ggplot2 (version 3.4.1) [51]. KEGG annotations were generated for the whole genome and used to identify statistically significant overrepresentations of specific KEGG terms among differentially expressed genes using Fisher's exact tests in R using an FDR cutoff of 0.01 [52].

Results

BAC MIC in FSL-N1-304 and mutants

The BAC MIC for FSL-N1-304 was measured in both liquid culture and solid media to establish a baseline MIC for all subsequent screening steps. All experiments were performed in triplicate and averaged to calculate the baseline MIC. In the liquid culture assay, the BAC MIC for the WT strain was $4\ \mu\text{g/ml}$ (Fig 2A). For the solid media assay, the BAC MIC was $3\ \mu\text{g/ml}$ (Fig 2B). During our mutant screening, we isolated two mutants with increased tolerance to BAC (*mut-1* and *mut-2*). *mut-1* and *mut-2* displayed BAC MICs of $7\ \mu\text{g/ml}$ in liquid culture, and 4 and $5\ \mu\text{g/ml}$ in solid culture, respectively (Fig 2A and 2B). We also measured the growth kinetics of the WT, *mut-1*, and *mut-2* in the presence of 0, 2, and $3\ \mu\text{g/ml}$ BAC in liquid TSB+YE media over the course of 48 hours. Under BAC stress, we observed diminished growth and an extended lag phase in the WT compared to *mut-1* and *mut-2* (Fig 3). Notably, WT, *mut-1* and *mut-2* had nearly identical growth patterns in TSB+YE (Fig 3), suggesting there is no growth tradeoff in the absence of BAC in the mutant strains.

BAC tolerant mutants show increased tolerance to some antibiotics

Previous studies showed that BAC tolerant *L. monocytogenes* isolates often also showed increased tolerance to some antibiotics [22,24]. To test whether this phenomenon was observed in our BAC tolerant mutants, we measured the MIC of ciprofloxacin, gentamicin, erythromycin, ampicillin, tetracycline, norfloxacin, penicillin G, and vancomycin in the WT and mutant strains (Fig 4 and Table 1). The MICs for erythromycin, ampicillin, tetracycline and penicillin G in the WT and mutants were either identical, decreased in the mutants, or showed a minor increase in the mutants but would still be considered "sensitive" to the antibiotic based on *Staphylococcus* spp. MIC breakpoints [33]. Additionally, we observed a near doubling of vancomycin MIC from $0.44\ \mu\text{g/ml}$ in the WT to 0.75 and $0.875\ \mu\text{g/ml}$ in *mut-1* and *mut-2*, respectively, and an increase in gentamicin MIC from $1.25\ \mu\text{g/ml}$ to $4\ \mu\text{g/ml}$ in *mut-2* (Fig 4A and Table 1). The mutant vancomycin and gentamicin MICs are still considered "sensitive" to the antibiotics, based on MIC breakpoints for other species. For ciprofloxacin, we observed an increase in MIC from $0.5\ \mu\text{g/ml}$ in the WT to $2\ \mu\text{g/ml}$ in *mut-1*, which is considered "intermediate" tolerance (Table 1 and Fig 4B). Lastly, we observed a substantial increase in norfloxacin MIC from $2.5\ \mu\text{g/ml}$ in the WT to 16 and $8\ \mu\text{g/ml}$ in *mut-1* and *mut-2*, respectively (Table 1 and Fig 4B). Norfloxacin MICs of 8 and $16\ \mu\text{g/ml}$ are considered "intermediate" and "resistant", respectively.

Assessing virulence potential through hemolytic assay

To test whether the BAC tolerant phenotype is linked with *L. monocytogenes* virulence, we measured *hly* activity, an essential component of virulence, in the WT and mutant strains. *hly* activity was measured as the percent of hemolysis in goat blood. The parental strain had an

A

	Benzalkonium chloride concentration ($\mu\text{g/ml}$)							
	0	1	2	3	4	5	6	7
WT-1	0.69	0.46	0.49	0.48	0.00	0.00	0.00	0.00
WT-2	0.70	0.33	0.46	0.48	0.03	0.00	0.00	0.01
WT-3	0.63	0.28	0.46	0.46	0.04	0.01	0.01	0.00
<i>mut-1.1</i>	0.60	0.40	0.35	0.40	0.38	0.41	0.34	0.00
<i>mut-1.2</i>	0.48	0.35	0.33	0.34	0.34	0.40	0.38	-0.01
<i>mut-1.3</i>	0.42	0.32	0.33	0.35	0.33	0.40	0.33	-0.01
<i>mut-2.1</i>	0.52	0.35	0.28	0.33	0.27	0.30	0.31	-0.01
<i>mut-2.2</i>	0.65	0.60	0.57	0.40	0.39	0.37	0.34	-0.01
<i>mut-2.3</i>	0.56	0.34	0.23	0.27	0.24	0.31	0.30	-0.01

B

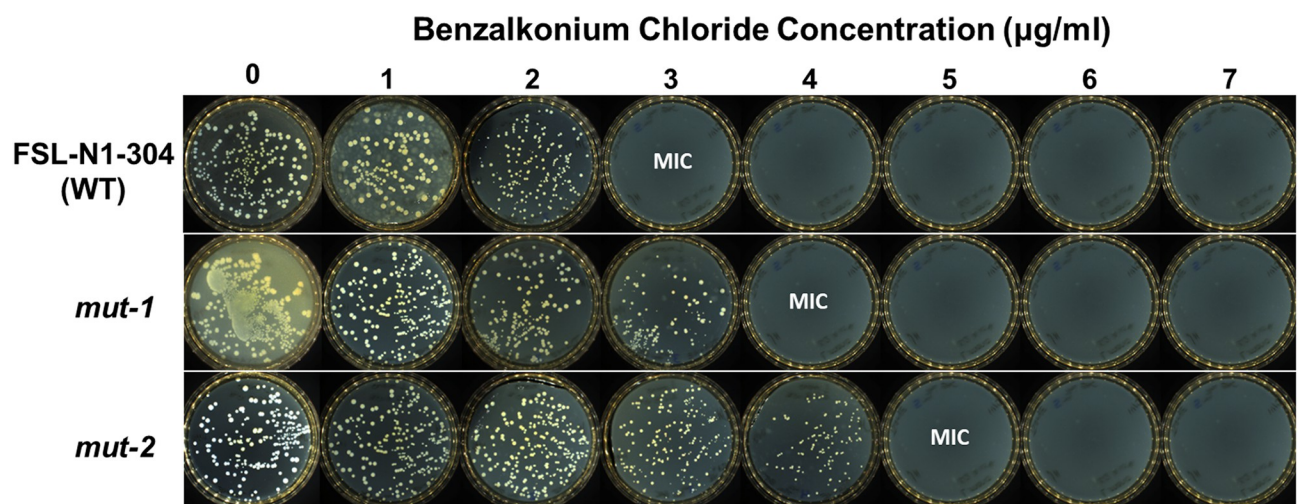


Fig 2. Minimum inhibitory concentration of benzalkonium chloride in WT and mutant *L. monocytogenes* strains. A) Columns represent samples (WT, *mut-1* and *mut-2*) and biological replicates, whole rows show the concentration ($\mu\text{g/ml}$) of benzalkonium chloride. Each component of the matrix shows the OD value after overnight growth. Growth was considered entirely inhibited when OD values < 0.1 . The red shading represents OD value, with light and dark red representing low and high OD values. B) Minimum inhibitory concentrations of *L. monocytogenes* WT and mutants to benzalkonium chloride on solid media. 100 μl of overnight culture from the WT, *mut-1* and *mut-2* was spread onto TSA+YE plates with 0, 1, 2, 3, 4, 5, 6, and 7 $\mu\text{g/ml}$ benzalkonium chloride and incubated at 37°C for 24 hours. Plates were then imaged on an Interscience Scan1200. Benzalkonium chloride minimum inhibitory concentration (MIC) was determined as the concentration at which no colonies were visible.

<https://doi.org/10.1371/journal.pone.0305663.g002>

average hemolysis of 6.05%, while *mut-1* and *mut-2* had significantly higher hemolysis activities of 67.71% (p-value = 0.00093) and 45.45% (p-value = 0.012), respectively (Fig 5).

Genomic analysis of mutants

To investigate the EMS induced mutations that may account for the increased tolerance to BAC and antibiotics, we generated a complete genome assembly for FSL-N1-304 using Illumina and ONT sequencing and predicted genes and functional annotations (NCBI SRA run accession numbers SRR17006605 and SRR17067427 for the Illumina and ONT data, respectively). The genome was assembled into two contigs consisting of the genome (~3 Mb) and a plasmid (pLIS10–63.8Kbp) with a total of 3,033 protein coding genes (NCBI accession number

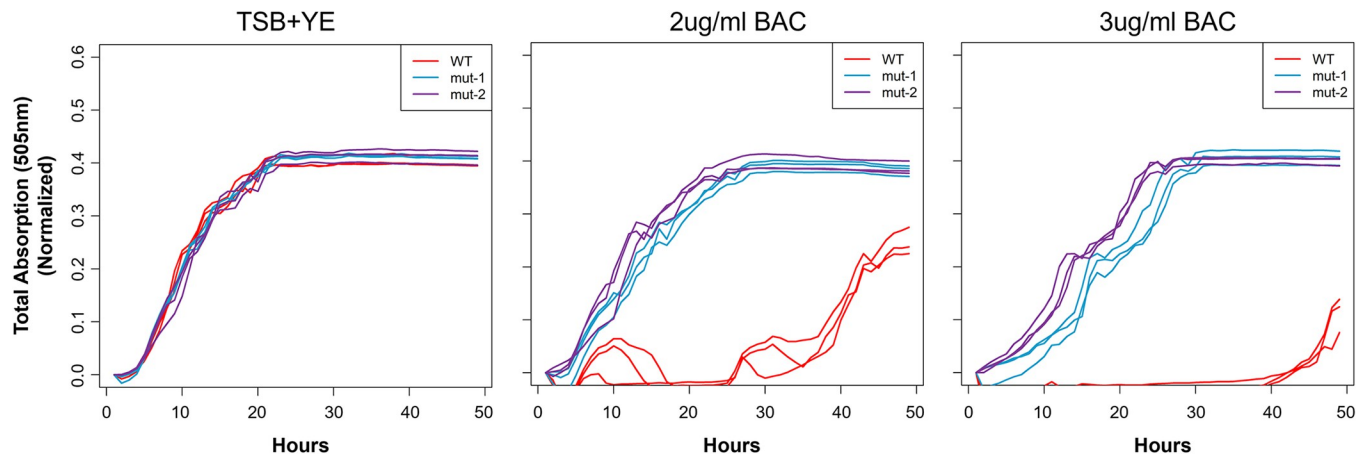


Fig 3. Growth rate analysis of WT, *mut-1*, and *mut-2* in response to increasing concentrations of benzalkonium chloride. Each culture was grown at room temperature for 48 hr and the growth rate was measured using the oCelloScope. (A) Growth curve of WT and mutant strains based on the total absorption (505nm wavelength) values in each microtiter well. (B) Growth curve of WT and mutant strains based on background corrected absorption (BCA) values. Growth rate was measured in 3 biological replicates for each sample. WT, *mut-1*, and *mut-2* are depicted by red, light blue and purple lines, respectively.

<https://doi.org/10.1371/journal.pone.0305663.g003>

GCA_021391455.1). This high-quality genome was used as a reference to map Illumina whole-genome resequencing data for *mut-1* and *mut-2*. We identified 3 and 29 mutations in the *mut-1* and *mut-2* genomes, respectively. For *mut-1*, consistent with EMS resulting mainly in G:C>A:T transitions, we observed three G>A missense mutations in genes with predicted functions as a diacylglycerol kinase, a permease, and a resuscitation-promoting factor (Table 2; Fig 6). In *mut-2*, we observed seven C>T transitions, 20 G>A transitions, one G>T transversion, and one single nucleotide deletion (Table 2). Twenty two of the 29 mutations in *mut-2* were missense mutations, three resulted in premature stop codon mutations, and a single nucleotide

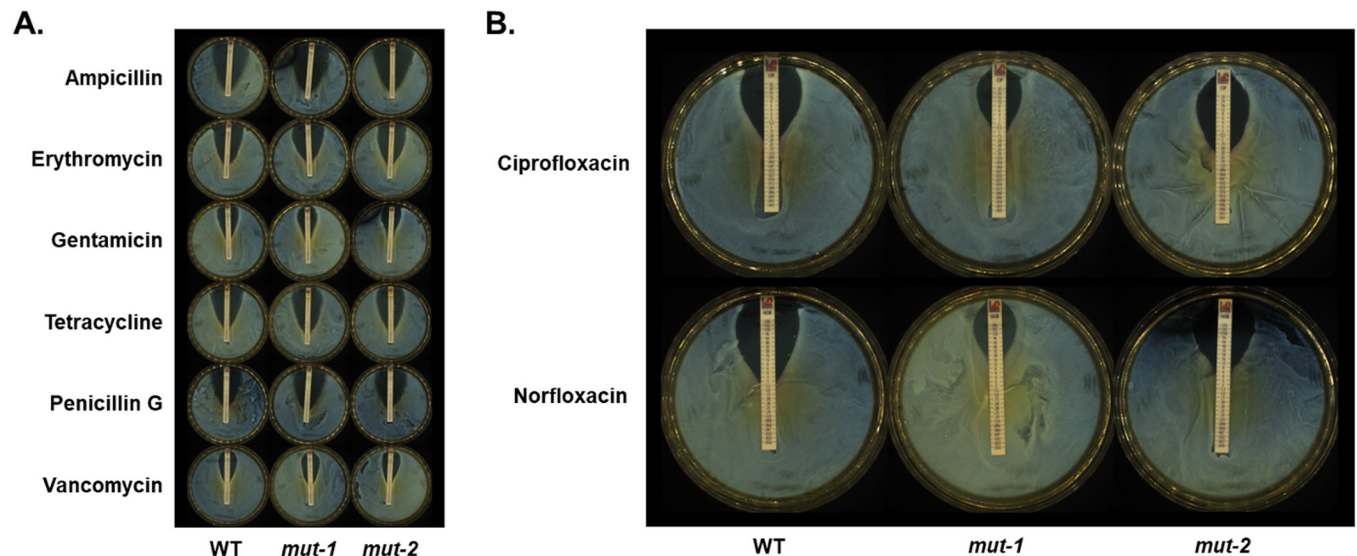


Fig 4. Minimum inhibitory concentrations of various antibiotics in the wild type and mutants with increased tolerance to benzalkonium chloride. The minimum inhibitory concentrations of ampicillin, erythromycin, gentamicin, tetracycline, penicillin G, and vancomycin (A) and the fluoroquinolones, ciprofloxacin and norfloxacin (B) were measured in the WT, *mut-1* and *mut-2* using Liofilchem Minimum inhibitory test strips. 10^9 CFU/ml cells were spread onto the TSA-YE plates and incubated at 37°C for 24 hours to create a lawn. The minimum inhibitory concentration was determined as the point where the edge of the inhibition ellipse intersected with the MIC Test Strip.

<https://doi.org/10.1371/journal.pone.0305663.g004>

Table 1. Minimum inhibitory concentrations of antibiotics for the WT, *mut-1* and *mut-2*, calculated as the average of two replicates.

Antibiotic	WT MIC ($\mu\text{g/ml}$)	<i>mut-1</i> MIC ($\mu\text{g/ml}$)	<i>mut-2</i> MIC ($\mu\text{g/ml}$)	Antibiotic breakpoint for <i>Staphylococcus</i>
Ampicillin	0.055	0.016	0.055	≥ 0.5
Erythromycin	0.315	0.315	0.22	≥ 0.8
Gentamycin	1.25	1.5	4*	≥ 16
Penicillin G	0.035	0.035	0.0275	≥ 0.25
Tetracycline	0.157	0.1875	0.1875	≥ 16
Vancomycin	0.44	0.75	0.875	≥ 16
Ciprofloxacin	0.5	2* (I)	0.5	≥ 4
Norfloxacin	2.5	16** (R)	8* (I)	≥ 16

(I): Value qualified as intermediate resistance as defined by the CLSI minimum inhibitory concentration breakpoints for *Staphylococcus* spp.

(R): Value qualified as resistant as defined by the CLSI minimum inhibitory concentration breakpoints for *Staphylococcus* spp.

* ≥ 2 -fold increase in MIC compared to WT.

** ≥ 4 -fold increase in MIC compared to WT.

<https://doi.org/10.1371/journal.pone.0305663.t001>

deletion resulted in a frameshift mutation (Table 2). Interestingly, none of the genes with mutations in *mut-1* and *mut-2* overlapped, suggesting different mechanisms of increased BAC tolerance.

Additionally, we investigated whether gene gain or loss in the mutants may have changed after mutagenesis using the LS-BSR pipeline [46]. Consistent with predictions from EMS mutagenesis, we did not detect any gene gains or losses in *mut-1* or *mut-2*, suggesting that structural variants did not influence the increase in BAC tolerance.

Differential gene expression analysis between WT and BAC-tolerant mutants

We performed RNA-sequencing of the WT, *mut-1* and *mut-2* in biological triplicates during growth in TSB+YE containing 2 $\mu\text{g/ml}$ BAC for 10 hours (mid-log phase) to examine transcriptome profile differences across samples. We performed principal component analysis (PCA) of DESeq2 normalized read counts (Fig 7C). Biological replicates for each sample clustered together, suggesting the biological replicates had similar transcriptome profiles, and that there are major differences in the transcriptome response to BAC across samples. We independently identified differentially expressed genes in *mut-1* and *mut-2* relative to the WT. We identified 282 up-regulated genes and 134 down-regulated genes in *mut-1*, and 136 up-regulated and 45 down-regulated genes in *mut-2* (Fig 7). *mut-1* and *mut-2* share 55 up-regulated genes and 15 down-regulated genes (S1 and S2 Figs). Genes of the phosphotransferase system (PTS) (including *bglG*, *dhaL*, *dhaM*, *ulaA*, *fruA*, *manZ*, and *licABC*) were up-regulated in both *mut-1* and *mut-2* compared to the WT. KEGG pathway enrichment analysis supported this observation, revealing that KEGG terms corresponding to the PTS were overrepresented amongst all up-regulated genes in both *mut-1* (p-value = 0.000452) and *mut-2* (p-value = 0.00112). Additionally, two internalin-encoding genes, *inlB* and *inlH*, the *groEL-groES* chaperonin system, transcriptional antiterminator *lmo0425*, and multidrug transporter *lmo2463* were all up-regulated in both *mut-1* and *mut-2*. Interestingly, KEGG pathway enrichment analysis also revealed that genes involved in amino acid biosynthesis were overrepresented in the up-regulated genes of *mut-1*, while amino acid metabolism was overrepresented in up-regulated genes of *mut-2* (S3 and S4 Figs).

We identified *fepR*, the negative regulator of the efflux pump *fepA*, in the subset of genes down-regulated in both *mut-1* and *mut-2* (Fig 7A and 7B). Interestingly, despite the down-

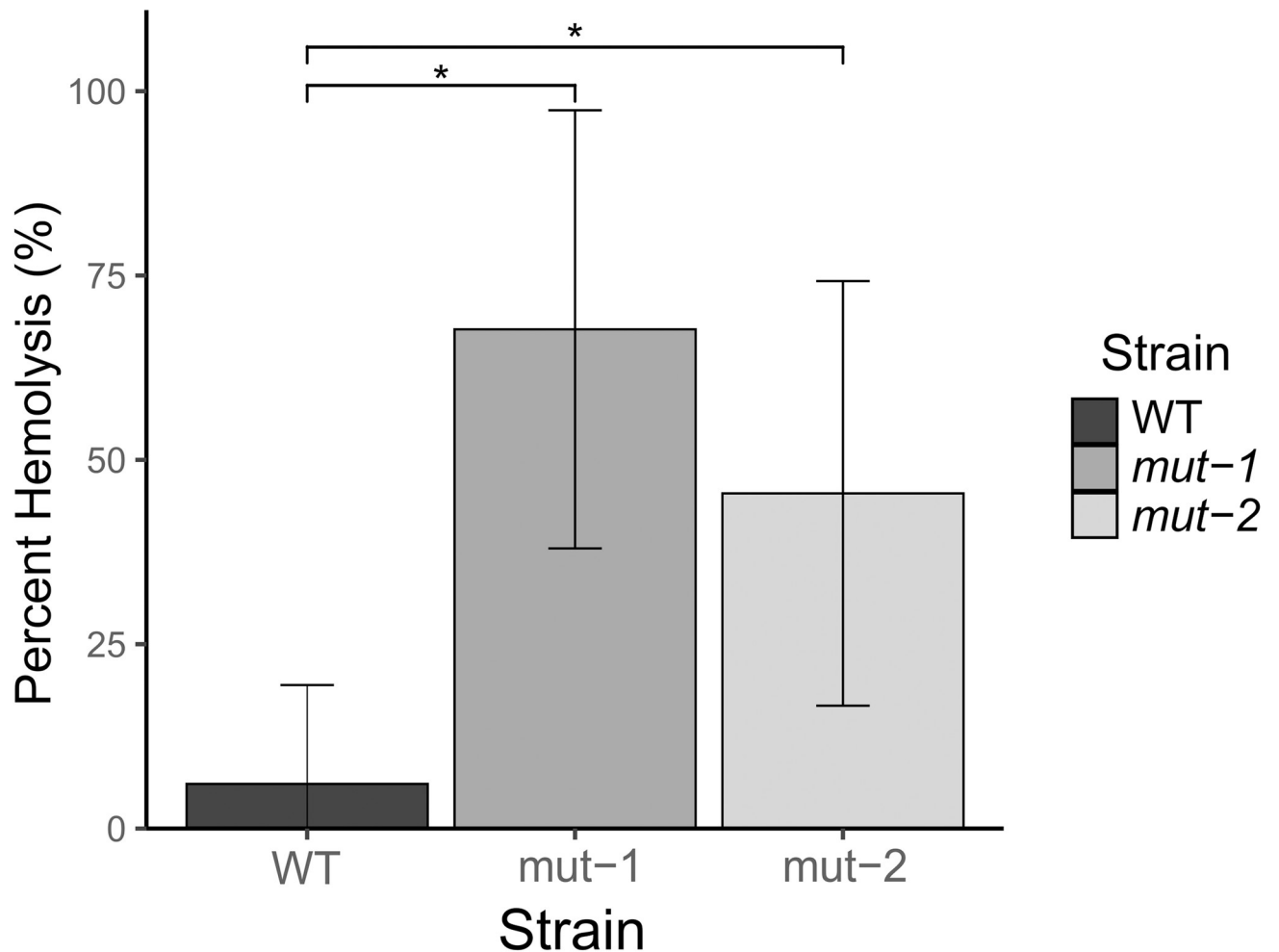


Fig 5. Hemolytic activity is significantly increased in BAC-tolerant mutants. To investigate the relationship between BAC tolerance and virulence, we conducted a hemolysis assay using *mut-1*, *mut-2*, and the parental strain. Percent hemolysis, which is a semi-quantitative proxy for the expression of key *L. monocytogenes* virulence factor listeriolysin O is reported. Error bars represent the standard deviation of percent hemolysis for each lineage. Statistically significant values between WT, *mut-1* (p-value = 0.00093), and *mut-2* (p-value = 0.012) are indicated by an asterisk.

<https://doi.org/10.1371/journal.pone.0305663.g005>

regulation of *fepR*, we found that *fepA* was highly down-regulated (LFC = -3.05, p-value = 0) in *mut-2*. We also observed transcriptome profile differences between the two mutants in the *ilv-leu* operon, which is highly up-regulated only in *mut-1* (*leuA*—LFC = 2.35, p-value = 2.91E-08; *leuB*—LFC = 2.52, p-value = 2.15E-13; *leuC*—LFC = 2.40, p-value = 1.28E-12; *leuD*—LFC = 2.46, p-value = 7.07E-14; *ilvA*—LFC = 2.26, p-value = 5.63E-34; *ilvB*—LFC = 1.82,

Table 2. Description of genetic variants identified from comparative genomic analysis of WT, *mut-1*, and *mut-2*. Nucleotide base substitutions are displayed to demonstrate the G to A and C to T transitions that are characteristic of EMS mutagenesis. UniProtKB, BioCyc, and NCBI BLAST databases were used to annotate all genes and their corresponding protein products.

Mutant	Gene ID	WT allele	mut allele	Mutation	Gene Name	Annotation
<i>mut-1</i>	MEAOLCCM_00593	G	A	p. His245Tyr	<i>dagK</i>	Diacylglycerol kinase
	MEAOLCCM_01768	G	A	p.Pro60Ser	<i>lmo2768</i>	Permease
	MEAOLCCM_02042	G	A	p. Glu202Lys	<i>lmo0186</i>	Resuscitation-promoting factor

(Continued)

Table 2. (Continued)

Mutant	Gene ID	WT allele	mut allele	Mutation	Gene Name	Annotation
<i>mut-2</i>	MEAOLCCM_00152	C	T	p. Pro353Ser	<i>xseA</i>	Exodeoxyribonuclease 7 large subunit
	MEAOLCCM_00294	G	A	p.Ser82Phe	<i>udk</i>	Uridine kinase
	MEAOLCCM_00401	C	T	UGV	<i>lmo1597</i>	Hypothetical protein
	MEAOLCCM_00412	C	T	p.Val150Ile	<i>pheT</i>	PheT protein
	MEAOLCCM_00708	G	A	p.Thr139Ile	<i>msrA</i>	Peptide methionine sulfoxide reductase MsrA
	MEAOLCCM_00742	C	T	p. Ala148Val	<i>ponA</i>	Penicillin-binding protein 1A/1B
	MEAOLCCM_00894	G	A	p.Pro29Ser	<i>murG</i>	UDP-N-acetylglucosamine—N-acetylmuramyl-(pentapeptide) pyrophosphoryl-undecaprenol N-acetylglucosamine transferase
	MEAOLCCM_00905	G	A	UGV	<i>lmo2045</i>	Hypothetical protein
	MEAOLCCM_00932	G	A	p.Tyr25Tyr	<i>rex</i>	Redox-sensing transcriptional repressor Rex
	MEAOLCCM_01029	G	T	UGV	<i>lmo2085</i>	Peptidoglycan binding protein
	MEAOLCCM_01142	G	A	p.Arg150*	<i>pepF</i>	Oligoendopeptidase F plasmid
	MEAOLCCM_01207	G	A	p. Gly229Ser	<i>aspB</i>	Asparagine—oxo-acid transaminase
	MEAOLCCM_01289	G	A	p. Val486Val	<i>mrpA</i>	Na(+)/H(+) antiporter subunit A
	MEAOLCCM_01298	G	A	p. Gly124Asp	<i>yfeO</i>	Putative ion-transport protein YfeO
	MEAOLCCM_01398	G	A	p.Gln359*	<i>uvrB</i>	UvrABC system protein B
	MEAOLCCM_01420	G	A	p. Ser139Leu	<i>hpf</i>	Ribosome hibernation promotion factor
	MEAOLCCM_01494	G	A	UGV	<i>hssS</i>	Heme sensor protein HssS
	MEAOLCCM_01544	G	A	p.Gln113*	unknown	YopX family protein
	MEAOLCCM_01547	TCTTTACTTTCTTTACTTTCC	TCTTTACTTTCC	frameshift	unknown	Hypothetical protein
	MEAOLCCM_01628	G	A	p. Lys135Lys	<i>lmo2638</i>	NADH dehydrogenase
	MEAOLCCM_01686	G	A	p. Ala226Val	<i>speA</i>	Arginine decarboxylase
	MEAOLCCM_01991	C	T	p. Glu398Glu	<i>lmo0130</i>	Cell wall protein
	MEAOLCCM_02285	C	T	p.Ser486Ser	<i>inlA</i>	Internalin A
	MEAOLCCM_02368	C	T	p. Ser244Leu	<i>lmo0501</i>	BglG family transcription antiterminator
	MEAOLCCM_02534	G	A	p.Gly87Asp	<i>ssbA</i>	Single-stranded DNA-binding protein A
	MEAOLCCM_02864	G	A	p. Asp435Asn	<i>licR</i>	putative licABCH operon regulator
	MEAOLCCM_02969	G	A	p. Gly112Asp	<i>cutC</i>	Copper homeostasis protein CutC
	MEAOLCCM_03024	G	A	p.Ser504Ser	<i>pycA</i>	Pyruvate carboxylase
	MEAOLCCM_03069	G	A	p.Val214Ile	<i>lmo1135</i>	Immunity 26/phosphotriesterase HocA family protein

WT allele = wild-type allele, mut allele = mutant allele, mutation = mutation in protein, UGV = upstream gene variant.

<https://doi.org/10.1371/journal.pone.0305663.t002>

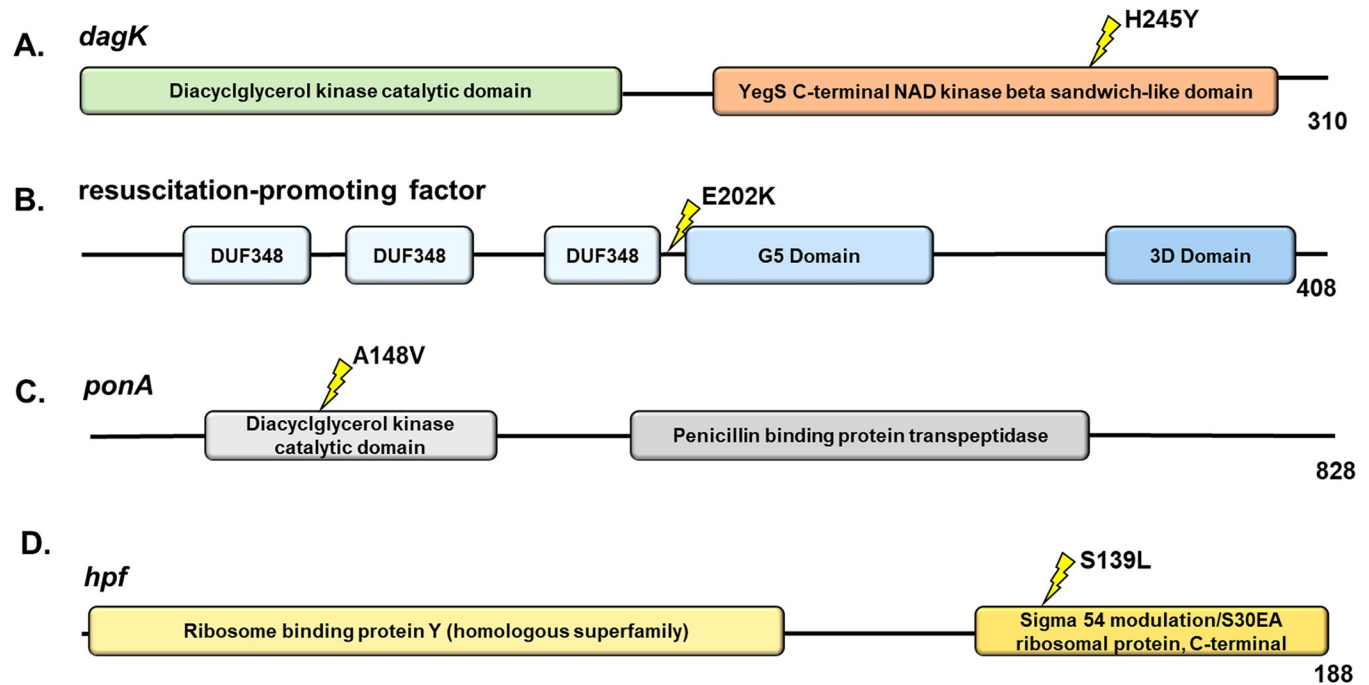


Fig 6. Candidate proteins in mutants with increased resistance to benzalkonium chloride. The common *L. monocytogenes* gene name is provided for each protein. InterPro functional domains are represented by colored ellipses. The yellow lightning bolt symbol represents the site of the nonsynonymous mutations. (A and B) *dagK* (locus tag: LZJ96_02845) and resuscitation-promoting factor (LZJ96_09855) mutations were present in *mut-1*, while (C and D) *ponA* (LZJ96_03560) and *hpf* (LZJ96_06860) mutations were present in *mut-2*. The number at the end of the protein represents the length of the protein in amino acids.

<https://doi.org/10.1371/journal.pone.0305663.g006>

p-value = 3.32E-06; *ilvC*—LFC = 2.27, p-value = 2.12E-09; *ilvH*—LFC = 2.02, p-value = 1.76E-08). The *ilv-leu* operon is involved in branched-chain amino acid synthesis and has been associated with *L. monocytogenes* survival under harsh, host-associated conditions [53,54]. Only four of the candidate genes with mutations in either *mut-1* or *mut-2* were differentially expressed (*mut-1*: *lmo0186* and *mut-2*: *rex*, *yfeO*, *hpf*).

Discussion

Here, we used EMS mutagenesis to generate *L. monocytogenes* mutants with increased tolerance to BAC in an effort to understand the potential genetic underpinnings and transcriptome response to BAC tolerance, and the off-target effects of BAC tolerance on antibiotic sensitivity. We conducted this study with *L. monocytogenes* FSL-N1-304 because this strain lacks genomic elements, such as *bcrABC*, *qacH* and *Tn6188*, which are involved in QAC resistance [55–57]. For instance, analysis of over 116 *L. monocytogenes* isolates from diverse serotypes and origins revealed that 71 of the 72 strains displaying BAC resistance harbored *bcrABC* [55], while another study showed that strains harboring *Tn6188* have BAC MICs twice as high as strains lacking *Tn6188* [57]. Thus, the isolation of FSL-N1-304 mutants displaying increased BAC tolerance could reveal novel genetic elements and mechanisms involved in BAC tolerance.

We generated two mutants with elevated BAC MICs in both liquid and solid media compared to the parental FSL-N1-304 strain (Figs 2 and 3). Additionally, *mut-1* and *mut-2* harbored resistance and increased tolerance to norfloxacin, respectively, while the parental FSL-N1-304 strain was sensitive to the antibiotic (Table 1 and Fig 4B). We sequenced the genomes of the WT, *mut-1* and *mut-2* to identify candidate mutations involved in increased BAC tolerance. Interestingly, the number of mutations we observed between our two mutants

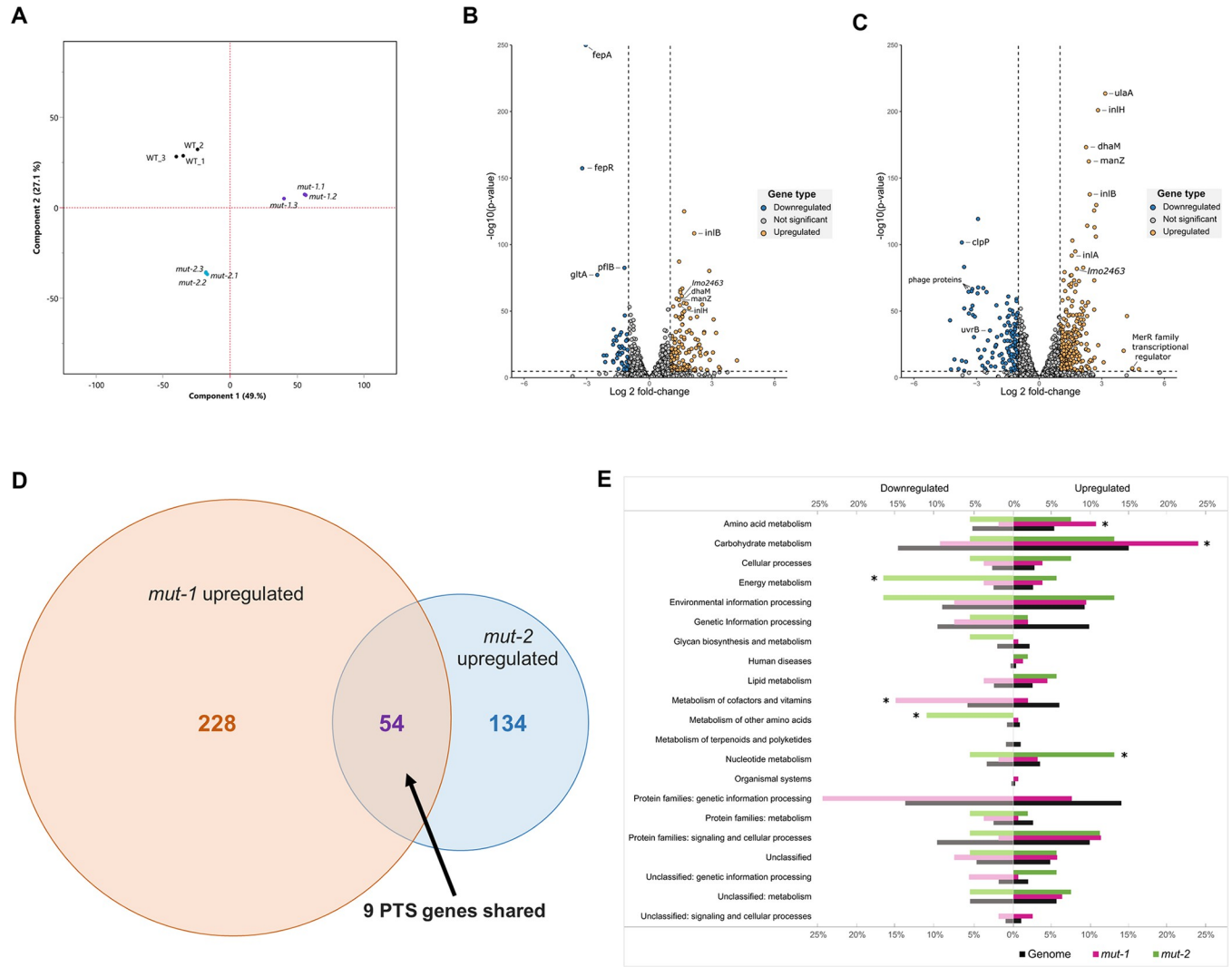


Fig 7. Transcriptome response to BAC stress in WT and mutants. (A) Principal component analysis of RNA-sequencing data reveals distinct clustering of WT and mutant strains. PCA was conducted on genome-wide normalized DESeq2 read counts. *mut-1* and *mut-2* replicates are displayed using purple dots and light blue dots, respectively. WT replicates are represented with black dots. (B and C) Volcano plots displaying differential gene expression analysis results for *mut-1* (B) and *mut-2* (C) show differential gene expression of mutants relative to the parental strain. Vertical dashed lines represent differential expression thresholds, which were defined using log-fold change [log₂(FC)] values >1 (up-regulated) and <-1 (down-regulated). The horizontal dashed line represents the significance threshold defined using a multiple test corrected p-value: (significance level)/(total # of genes) = 0.05/3201 = 1.6E-5. (D) Venn diagram comparison of all up-regulated genes identified in *mut-1* and *mut-2*. The PTS accounted for 9 out of 52 (16.67%) shared up-regulated genes. (E) Enrichment of KEGG terms among differentially expressed genes. The proportion of genes belonging to each functional category within (1) the total WT genome, (2) differentially expressed genes in *mut-1*, and (3) differentially expressed genes in *mut-2* correspond to black, pink, and green bars, respectively. Asterisks indicate significant overrepresentations (p-value < 0.01).

<https://doi.org/10.1371/journal.pone.0305663.g007>

differed by an order of magnitude (Table 2). In two recent EMS mut-seq studies in *L. monocytogenes*, 1 to 6 mutations were observed per mutant [58,59]. *mut-2* contained 29 mutations, and the majority of these mutations were in G:C > A:T transitions, consistent with expectations from EMS mutagenesis. However, we observed a mutation in *uvrB* (which encodes the nucleotide excision repair enzyme UvrABC system protein B) that results in a premature stop codon and truncated protein that lacks the C-terminus helicase C, UvrB_YAD/RRR_dom, and UVR_dom domains (Table 2). This mutation is likely responsible for the higher number of mutations observed in *mut-2*.

mut-1 contained only three nonsynonymous mutations that differentiate it from the parental FSL-N1-304 strain. One of these mutations occurred in *dagK* (*lmo1753*), a gene encoding a diacylglycerol kinase (DAGK) (Fig 6A). In a previous study investigating *L. monocytogenes* adaptation to QACs, mutations were observed in *lmo1753* in all QAC-tolerant strains, leading the authors to hypothesize that *lmo1753* mutations contribute to QAC tolerance by altering fatty acid composition [60]. Membrane modifications and increased hydrophobicity has been previously identified as a putative mechanism of BAC resistance in *L. monocytogenes* [61–63]. In *E. coli*, DAGK recycles diacylglycerol that is produced by membrane-derived oligosaccharide biosynthesis [64]. Interestingly, in *Acinetobacter baumannii*, *dagK* was significantly up-regulated in a colistin-resistant strain compared to its colistin-susceptible parental strain [65]. Both colistin and BAC disrupt the membrane, and alterations to expression or structure may improve cell membrane integrity, underlying a potential mechanism for increased BAC tolerance in *mut-1*. Additionally, *mut-1* contained a nonsynonymous mutation in a predicted permease encoding gene (Table 2). The P60S mutation is predicted to occur outside the membrane in the extracellular region. Lastly, we observed a mutation in a gene encoding a predicted resuscitation-promoting factor that is also annotated in the Gene Ontology category peptidoglycan turnover (GO:0009254) (Fig 6B). As a gram-positive bacterium, the *L. monocytogenes* cell wall is composed of a rigid layer of peptidoglycan that acts as a barrier to the external environment. It has previously been hypothesized that modifications to peptidoglycan synthesis could alter membrane fluidity and could be involved in BAC resistance [21].

Though linking mutations to the increased BAC tolerance phenotype in *mut-2* is more challenging because of the relatively large number of mutations observed, we identified several interesting candidates. *mut-2* contained a nonsynonymous mutation (A148V) in the penicillin-binding protein (PBP) encoding gene, *ponA* (Fig 6C). This protein is involved in polymerizing and modifying peptidoglycan, making it an interesting candidate for the BAC tolerance phenotype. While PBPs have not been implicated in QAC resistance, their presence has been associated with *L. monocytogenes* resistance to β -lactam antibiotics [66]. Additionally, we observed a nonsynonymous mutation (S139L) in the gene encoding for the ribosome hibernation promotion factor (HPF) (Fig 6D). In *L. monocytogenes*, *hpf* knockout mutants showed greater uptake of gentamicin and generally, were more sensitive to aminoglycosides during stationary phase [67]. This mutation is an interesting candidate, as we observed an increase in gentamicin MIC from 1.25 $\mu\text{g}/\text{ml}$ in the parental strain to 4 $\mu\text{g}/\text{ml}$ in *mut-2* (Fig 4A, Table 1). Additionally, *L. monocytogenes* strains harboring plasmid pLMST6, which contains *emrC*, a multidrug efflux pump transporter, showed increased tolerance to both BAC and gentamicin [68], suggesting increased tolerance to these compounds may be achieved through similar paths.

We hypothesized that there are two separate efflux mechanisms acting as contributors to the decreased antimicrobial susceptibility observed in these mutants because the transcriptome profiles of the two mutants reveal differential expression of *fepR* and *lmo2463*. *fepR* encodes a transcriptional regulator that negatively regulates its downstream target, FepA, a multi-drug efflux pump that is linked to both QAC and fluoroquinolone resistance [24,25,69]. One study showed that a loss-of-function frameshift mutation in *fepR* resulted in up-regulation of *fepA* and subsequent resistance to norfloxacin and ciprofloxacin [27]. Another study experimentally evolved *L. monocytogenes* for increased tolerance to BAC and didecyldimethyl ammonium chloride and showed that these adapted lineages were also resistant to ciprofloxacin stemming mainly from missense and nonsense mutations in *fepR* [25]. Interestingly, the increased tolerance to ciprofloxacin was only observed in *mut-1* and was not as drastic as the increased MIC for norfloxacin (Fig 4B). We did not observe mutations in *fepR* or *fepA* in the mutants, which initially suggested that the increased tolerance to BAC and fluoroquinolones occurred through

pathways independent of the *fepR/fepA* genotype. However, our RNA-seq results suggest that the *fepR/fepA* mechanism may be still contributing to the BAC mutant phenotypes. *fepR* was down-regulated in both mutants in the presence of BAC, albeit the relative expression was considerably lower in *mut-2* compared to *mut-1* (*mut-1*: $\log_2[\text{FC}] = -3.22$ and *mut-2*: $\log_2[\text{FC}] = -1.03$). Despite down-regulation of its negative repressor in both *mut-1* and *mut-2*, surprisingly, *fepA* was significantly down-regulated in *mut-1*, and not significantly differentially expressed in *mut-2* (Fig 7). Previously work had shown that increased BAC tolerance is often associated with up-regulation of *fepA*. However, in the present study, *fepA* is down-regulated in the BAC-tolerant *mut-1*, suggesting *fepA* and *fepR* independent mechanisms for BAC tolerance.

The second efflux pump mechanism that we hypothesize may be contributing to decreased antimicrobial susceptibility is the MmpL family transporter protein encoded by *lmo2463*. MmpL family transporters are a class of multi-drug resistance proteins that increase resistance to fluoroquinolones in *E. coli* [70]. Other studies have shown that MmpL family proteins were induced under acid stress in *L. monocytogenes* [71]. We found that *lmo2463* was up-regulated in both mutants when grown in the presence of BAC stress. Additionally, considering the increased tolerance to fluoroquinolone antibiotics compared to the WT, the MmpL transporter is a potential candidate of BAC and fluoroquinolone tolerance. Efflux pump deletion mutants will need to be generated in future work to determine if synergistic effects exist between *fepR/fepA* and the MmpL efflux mechanism.

Collectively, our results offer potential insight to the aforementioned hypothesis that variability in peptidoglycan synthesis contributes to BAC tolerance as we observed a significant up-regulation of genes of the PTS, which is involved in cell wall turnover and peptidoglycan modulation [21,72]. Enrichment analysis of KEGG pathways also revealed that *mut-1* and *mut-2* contained 20 and 14 up-regulated PTS genes, respectively. The PTS in *L. monocytogenes* (as well as other bacterial pathogens) is associated with tolerance mechanisms to various stressors including sanitizers and antibiotics [61,71,73–76]. Several PTS genes that were up-regulated in *mut-1* and *mut-2* are highlighted in Fig 7A and 7B, including *ulaA*, *dhaM*, and *manZ*. Another study on benzalkonium chloride tolerance in *L. monocytogenes* found that *manZ* mutations were only observed in benzalkonium-adapted strains, which provides further support that the PTS is heavily involved in biocide tolerance [25]. Further, an additional study demonstrated similar findings, observing that PTS genes were highly up-regulated in *L. monocytogenes* when exposed to benzethonium chloride (BZT), another QAC [61]. The PTS has other implications for stress tolerance as demonstrated by the disruption of the mannose-specific PTS operon *mpt* and overexpression of the *bgl* operon, which caused increased resistance to bacteriocins [74,75,77].

As shown in Fig 5, a significant increase in hemolytic activity was observed in both *mut-1* (p-value = 0.000931) and *mut-2* (p-value = 0.0125) compared to the WT, suggesting that increased BAC tolerance may be positively correlated to higher hemolytic activity. Additionally, several internalin-encoding genes involved in virulence, including *inlB* and *inlH*, were up-regulated in both *mut-1* (*inlB*—LFC = 2.42, p-value = 1.84E-138; *inlH*—LFC = 2.82, p-value = 1.01E-201) and *mut-2* (*inlB*—LFC = 2.15, p-value = 3.61E-109; *inlH*—LFC = 1.46, p-value = 4.25E-55) (Fig 7A and 7B). Expression of *inlH* has been previously shown to be associated with *L. monocytogenes* stress response, as it is under σ^B -dependent regulation [78]. Transcriptional analysis showed no significant difference in the expression of *hly* or other key virulence factors such as *prfA*, *actAB*, or *plcAB* under BAC stress. We did, however, observe significant up-regulation of the ATPase-encoding gene, *clpC* (*mut-1*: LFC = 1.58, p-value = 9.92E-104 and *mut-2*: LFC = 1.14, p-value = 3.79E-54), which has been previously associated with increased virulence and increased susceptibility to a variety of stressors [79,80]. In

mut-1, we also observed up-regulation of the *ilv-leu* operon, which is primarily associated with branched-chain amino acid synthesis but has also been shown to be under nutrient-dependent negative regulation by two virulence effectors, CodY and *Rli60* [53,54]. Overall, our observations suggest that the adaptive response to BAC stress may influence virulence determinants. Alternatively, mutations introduced during mutagenesis that are not involved in BAC tolerance could account for the observed increase in hemolysis.

Taken together, our work suggests that the emergence of adaptive mutations for BAC tolerance in *L. monocytogenes* isolates found in food processing facilities could also result in strains that are more virulent (Fig 5) and have increased tolerance to particular antibiotics (Table 1, Fig 4). While the mutants we isolated did not develop BAC resistance at levels that would enable survival at BAC concentrations used for sanitization in industry, environments such as floor drains may present scenarios in which sanitizers are diluted to sub-lethal concentrations, resulting in continued exposure and subsequent adaptation. For instance, a recent study in *L. monocytogenes* observed that sub-lethal short-term exposure (10 days) to BAC and didecyldimethylammonium chloride resulted in decreased susceptibility to ciprofloxacin [28]. Additionally, several adaptive laboratory evolution studies in which *Pseudomonas aeruginosa* or *E. coli* were grown in the presence of BAC have observed decreased sensitivity to BAC, and increased resistance to several unrelated antibiotics [81–83]. Thus, understanding the genetic underpinnings and consequences of BAC tolerance is vitally important for both controlling *L. monocytogenes* in the food processing environment and for preventing the spread of antibiotic resistance.

Supporting information

S1 Fig. UniProt BLAST annotation of genes that were up-regulated in both *mut-1* and *mut-2*.

(TIF)

S2 Fig. UniProt BLAST annotation of genes that were down-regulated in both *mut-1* and *mut-2*.

(TIF)

S3 Fig. KEGG term enrichment of up-regulated genes. KEGG terms were assigned for the whole genome and enrichment analysis was performed using Fisher's exact test to identify gene categories that were significantly up-regulated in the mutant strains (p-value < 0.01).

(TIF)

S4 Fig. KEGG term enrichment of down-regulated genes. KEGG terms were assigned for the whole genome and enrichment analysis was performed using Fisher's exact test to identify gene categories that were significantly down-regulated in the mutant strains (p-value < 0.01).

(TIF)

Author Contributions

Conceptualization: Tyler D. Bechtel, Julia Hershelman, John G. Gibbons.

Data curation: Tyler D. Bechtel, John G. Gibbons.

Formal analysis: Tyler D. Bechtel, Julia Hershelman, Mrinalini Ghoshal.

Funding acquisition: Lynne McLandsborough, John G. Gibbons.

Investigation: Tyler D. Bechtel, Julia Hershelman, John G. Gibbons.

Methodology: Tyler D. Bechtel, Julia Hershelman, Mrinalini Ghoshal, Lynne McLandsborough, John G. Gibbons.

Project administration: John G. Gibbons.

Resources: Mrinalini Ghoshal, Lynne McLandsborough, John G. Gibbons.

Software: John G. Gibbons.

Supervision: Tyler D. Bechtel, John G. Gibbons.

Validation: Tyler D. Bechtel.

Visualization: Tyler D. Bechtel, Julia Hershelman, John G. Gibbons.

Writing – original draft: Tyler D. Bechtel, Julia Hershelman, John G. Gibbons.

Writing – review & editing: Tyler D. Bechtel, Julia Hershelman, Mrinalini Ghoshal, Lynne McLandsborough, John G. Gibbons.

References

1. Farber JM, Peterkin PI. *Listeria monocytogenes*, a food-borne pathogen. *Microbiol Rev.* 1991; 55: 476–511. <https://doi.org/10.1128/mr.55.3.476-511.1991> PMID: 1943998
2. Ramaswamy V, Cresence VM, Rejitha JS, Lekshmi U, Dharsana KS, Prasad P, et al. *Listeria*-review of epidemiology and pathogenesis. *J Microbiol Immunol Infect.* 2007; 40: 4–13. PMID: 17332901
3. Clauss HE, Lorber B. Central Nervous System Infection with *Listeria monocytogenes*. 2008 [cited 19 Jan 2023]. Available: <http://www.cdc.gov/pulsenet/>.
4. Madjankov M, Chaudhry S, Ito S. Listeriosis during pregnancy. *Arch Gynecol Obstet.* 296. <https://doi.org/10.1007/s00404-017-4401-1>
5. Scallan E, Hoekstra RM, Angulo FJ, Tauxe R v., Widdowson MA, Roy SL, et al. Foodborne Illness Acquired in the United States—Major Pathogens. *Emerg Infect Dis.* 2011; 17: 7. <https://doi.org/10.3201/eid1701.p111101> PMID: 21192848
6. Townsend A, Strawn LK, Chapman BJ, Dunn LL. A Systematic Review of *Listeria* Species and *Listeria monocytogenes* Prevalence, Persistence, and Diversity throughout the Fresh Produce Supply Chain. *Foods* 2021, Vol 10, Page 1427. 2021;10: 1427. <https://doi.org/10.3390/foods10061427> PMID: 34202947
7. Farber JM, Zwietering M, Wiedmann M, Schaffner D, Hedberg CW, Harrison MA, et al. Alternative approaches to the risk management of *Listeria monocytogenes* in low risk foods. *Food Control.* 2021; 123: 107601. <https://doi.org/10.1016/j.foodcont.2020.107601>
8. Khandke SS, Mayes T. HACCP implementation: a practical guide to the implementation of the HACCP plan. *Food Control.* 1998; 9: 103–109. [https://doi.org/10.1016/S0956-7135\(97\)00065-0](https://doi.org/10.1016/S0956-7135(97)00065-0)
9. Pereira BMP, Tagkopoulos I. Benzalkonium Chlorides: Uses, Regulatory Status, and Microbial Resistance. *Appl Environ Microbiol.* 2019;85. <https://doi.org/10.1128/AEM.00377-19> PMID: 31028024
10. Jennings MC, Minbiole KPC, Wuest WM. Quaternary Ammonium Compounds: An Antimicrobial Mainstay and Platform for Innovation to Address Bacterial Resistance. *ACS Infect Dis.* 2015; 1: 288–303. <https://doi.org/10.1021/acsinfecdis.5b00047> PMID: 27622819
11. Wessels S, Ingmer H. Modes of action of three disinfectant active substances: a review. *Regul Toxicol Pharmacol.* 2013; 67: 456–467. <https://doi.org/10.1016/j.yrtph.2013.09.006> PMID: 24080225
12. Basaran P. Inhibition effect of benzalkonium chloride treatment on growth of common food contaminating fungal species. *J Food Sci Technol.* 2011; 48: 515. <https://doi.org/10.1007/s13197-011-0268-5> PMID: 23572782
13. Gelbicova T, Florianova M, Hluchanova L, Kalova A, Korena K, Strakova N, et al. Comparative Analysis of Genetic Determinants Encoding Cadmium, Arsenic, and Benzalkonium Chloride Resistance in *Listeria monocytogenes* of Human, Food, and Environmental Origin. *Front Microbiol.* 2021; 11: 3397. <https://doi.org/10.3389/fmicb.2020.599882> PMID: 33519740
14. Meier AB, Guldimann C, Markkula A, Pöntinen A, Korkeala H, Tasara T. Comparative Phenotypic and Genotypic Analysis of Swiss and Finnish *Listeria monocytogenes* Isolates with Respect to Benzalkonium Chloride Resistance. *Front Microbiol.* 2017;8. <https://doi.org/10.3389/FMICB.2017.00397> PMID: 28386248

15. Ratani SS, Siletzky RM, Dutta V, Yildirim S, Osborne JA, Lin W, et al. Heavy metal and disinfectant resistance of *Listeria monocytogenes* from foods and food processing plants. *Appl Environ Microbiol*. 2012; 78: 6938–6945. <https://doi.org/10.1128/AEM.01553-12> PMID: 22843526
16. Romanova NA, Wolffs PFG, Brovko LY, Griffiths MW. Role of efflux pumps in adaptation and resistance of *Listeria monocytogenes* to benzalkonium chloride. *Appl Environ Microbiol*. 2006; 72: 3498–3503. <https://doi.org/10.1128/AEM.72.5.3498-3503.2006> PMID: 16672496
17. Soumet C, Ragimbeau C, Maris P. Screening of benzalkonium chloride resistance in *Listeria monocytogenes* strains isolated during cold smoked fish production. *Lett Appl Microbiol*. 2005; 41: 291–296. <https://doi.org/10.1111/j.1472-765X.2005.01763.x> PMID: 16108923
18. Xu D, Li Y, Shamim Hasan Zahid M, Yamasaki S, Shi L, rong Li J, et al. Benzalkonium chloride and heavy-metal tolerance in *Listeria monocytogenes* from retail foods. *Int J Food Microbiol*. 2014; 190: 24–30. <https://doi.org/10.1016/j.ijfoodmicro.2014.08.017> PMID: 25173916
19. Hegstad K, Langsrud S, Lunestad BT, Scheie AA, Sunde M, Yazdankhah SP. Does the wide use of quaternary ammonium compounds enhance the selection and spread of antimicrobial resistance and thus threaten our health? *Microb Drug Resist*. 2010; 16: 91–104. <https://doi.org/10.1089/mdr.2009.0120> PMID: 20370507
20. Mc Carlie S, Boucher CE, Bragg RR. Molecular basis of bacterial disinfectant resistance. *Drug Resist Updat*. 2020;48. <https://doi.org/10.1016/j.drup.2019.100672> PMID: 31830738
21. To MS, Favrin S, Romanova N, Griffiths MW. Postadaptational resistance to benzalkonium chloride and subsequent physicochemical modifications of *Listeria monocytogenes*. *Appl Environ Microbiol*. 2002; 68: 5258–5264. <https://doi.org/10.1128/AEM.68.11.5258-5264.2002> PMID: 12406712
22. Yu T, Jiang X, Zhang Y, Ji S, Gao W, Shi L. Effect of Benzalkonium Chloride adaptation on sensitivity to antimicrobial agents and tolerance to environmental stresses in *Listeria monocytogenes*. *Front Microbiol*. 2018; 9: 2906. <https://doi.org/10.3389/fmicb.2018.02906> PMID: 30546352
23. Jiang X, Yu T, Xu Y, Wang H, Korkeala H, Shi L. MdrL, a major facilitator superfamily efflux pump of *Listeria monocytogenes* involved in tolerance to benzalkonium chloride. *Appl Microbiol Biotechnol*. 2019; 103: 1339–1350. <https://doi.org/10.1007/s00253-018-9551-y> PMID: 30539257
24. Guérin F, Galimand M, Tuambilangana F, Courvalin P, Cattoir V. Overexpression of the Novel MATE Fluoroquinolone Efflux Pump FepA in *Listeria monocytogenes* Is Driven by Inactivation of Its Local Repressor FepR. *PLoS One*. 2014; 9: e106340. <https://doi.org/10.1371/journal.pone.0106340> PMID: 25188450
25. Douarre PE, Sévellec Y, Le Grandois P, Soumet C, Bridier A, Roussel S. FepR as a Central Genetic Target in the Adaptation to Quaternary Ammonium Compounds and Cross-Resistance to Ciprofloxacin in *Listeria monocytogenes*. *Front Microbiol*. 2022; 13: 864576. <https://doi.org/10.3389/fmicb.2022.864576> PMID: 35663878
26. Kode D, Nannapaneni R, Bansal M, Chang S, Cheng WH, Sharma CS, et al. Low-level tolerance to fluoroquinolone antibiotic ciprofloxacin in qac-adapted subpopulations of *Listeria monocytogenes*. *Microorganisms*. 2021; 9: 1052. <https://doi.org/10.3390/microorganisms9051052> PMID: 34068252
27. Buffet-Bataillon S, Tattevin P, Maillard JY, Bonnaure-Mallet M, Jolivet-Gougeon A. Efflux pump induction by quaternary ammonium compounds and fluoroquinolone resistance in bacteria. *Future Microbiol*. 2016; 11: 81–92. <https://doi.org/10.2217/fmb.15.131> PMID: 26674470
28. Guérin A, Bridier A, Le Grandois P, Sévellec Y, Palma F, Félix B, et al. Exposure to Quaternary Ammonium Compounds Selects Resistance to Ciprofloxacin in *Listeria monocytogenes*. *Pathogens* 2021, Vol 10, Page 220. 2021;10: 220. <https://doi.org/10.3390/pathogens10020220> PMID: 33670643
29. Norton DM, Scarlett JM, Horton K, Sue D, Thimothe J, Boor KJ, et al. Characterization and Pathogenic Potential of *Listeria monocytogenes* Isolates from the Smoked Fish Industry. *Appl Environ Microbiol*. 2001; 67: 646. <https://doi.org/10.1128/AEM.67.2.646-653.2001> PMID: 11157227
30. Bose JL. Chemical and UV Mutagenesis. *Methods Mol Biol*. 2016; 1373: 111–115. https://doi.org/10.1007/7651_2014_190 PMID: 25646611
31. Haney EF, Trimble MJ, Hancock REW. Microtiter plate assays to assess antibiofilm activity against bacteria. *Nature Protocols* 2021 16:5. 2021; 16: 2615–2632. <https://doi.org/10.1038/s41596-021-00515-3> PMID: 33911258
32. SAMPATHKUMAR B, TSOUGRIANI E, YU LSL, KHACHATOURIANS GG. A quantitative microtiter plate hemolysis assay for *Listeria monocytogenes*. *J Food Saf*. 1998; 18: 197–203. <https://doi.org/10.1111/j.1745-4565.1998.tb00214.x>
33. Clinical and Laboratory Standards Institute. CLSI. Performance Standards for Antimicrobial Susceptibility Testing. 32nd ed. CLSI supplement M100. 32nd ed. 2022.
34. bcl2fastq: A proprietary Illumina software for the conversion of bcl files to basecalls. https://support.illumina.com/sequencing/sequencing_software/bcl2fastq-conversion-software.html.

35. Wick RR, Judd LM, Gorrie CL, Holt KE. Completing bacterial genome assemblies with multiplex MinION sequencing. *Microb Genom*. 2017; 3: e000132. <https://doi.org/10.1099/mgen.0.000132> PMID: 29177090
36. Wick RR, Judd LM, Gorrie CL, Holt KE. Unicycler: Resolving bacterial genome assemblies from short and long sequencing reads. *PLoS Comput Biol*. 2017; 13: e1005595. <https://doi.org/10.1371/journal.pcbi.1005595> PMID: 28594827
37. Gurevich A, Saveliev V, Vyahhi N, Tesler G. QUAST: quality assessment tool for genome assemblies. *Bioinformatics*. 2013; 29: 1072–1075. <https://doi.org/10.1093/bioinformatics/btt086> PMID: 23422339
38. Seemann T. Prokka: rapid prokaryotic genome annotation. *Bioinformatics*. 2014; 30: 2068–2069. <https://doi.org/10.1093/bioinformatics/btu153> PMID: 24642063
39. Martin M. Cutadapt removes adapter sequences from high-throughput sequencing reads. *EMBnet J*. 2011; 17: 10–12. <https://doi.org/10.14806/EJ.17.1.200>
40. Krueger F. “Trim galore” A wrapper tool around Cutadapt and FastQC to consistently apply quality and adapter trimming to FastQ files. 2015; 516.
41. Li H. Aligning sequence reads, clone sequences and assembly contigs with BWA-MEM. 2013 [cited 29 Jun 2022]. <https://doi.org/10.48550/arxiv.1303.3997>
42. Danecek P, Bonfield JK, Liddle J, Marshall J, Ohan V, Pollard MO, et al. Twelve years of SAMtools and BCFtools. *Gigascience*. 2021;10. <https://doi.org/10.1093/gigascience/giab008> PMID: 33590861
43. Garrison E, Marth G. Haplotype-based variant detection from short-read sequencing. 2012.
44. McKenna A, Hanna M, Banks E, Sivachenko A, Cibulskis K, Kernytsky A, et al. The Genome Analysis Toolkit: a MapReduce framework for analyzing next-generation DNA sequencing data. *Genome Res*. 2010; 20: 1297–1303. <https://doi.org/10.1101/gr.107524.110> PMID: 20644199
45. Cingolani P, Platts A, Wang LL, Coon M, Nguyen T, Wang L, et al. A program for annotating and predicting the effects of single nucleotide polymorphisms, SnpEff: SNPs in the genome of *Drosophila melanogaster* strain w1118; iso-2; iso-3. *Fly (Austin)*. 2012; 6: 80–92. <https://doi.org/10.4161/fly.19695> PMID: 22728672
46. Sahl JW, Gregory Caporaso J, Rasko DA, Keim P. The large-scale blast score ratio (LS-BSR) pipeline: a method to rapidly compare genetic content between bacterial genomes. *PeerJ*. 2014;2. <https://doi.org/10.7717/peerj.332> PMID: 24749011
47. Mitchell AL, Attwood TK, Babbitt PC, Blum M, Bork P, Bridge A, et al. InterPro in 2019: improving coverage, classification and access to protein sequence annotations. *Nucleic Acids Res*. 2019; 47: D351–D360. <https://doi.org/10.1093/nar/gky1100> PMID: 30398656
48. Quinlan AR, Hall IM. BEDTools: a flexible suite of utilities for comparing genomic features. *Bioinformatics*. 2010; 26: 841–842. <https://doi.org/10.1093/bioinformatics/btq033> PMID: 20110278
49. Love MI, Huber W, Anders S. Moderated estimation of fold change and dispersion for RNA-seq data with DESeq2. *Genome Biol*. 2014; 15: 1–21. <https://doi.org/10.1186/s13059-014-0550-8> PMID: 25516281
50. SAS Institute Inc. JMP® Pro. Cary, NC; pp. 1989–2023.
51. Wickham H. ggplot2: Elegant Graphics for Data Analysis. Springer-Verlag. 2016.
52. Kanehisa M, Goto S. KEGG: kyoto encyclopedia of genes and genomes. *Nucleic Acids Res*. 2000; 28: 27–30. <https://doi.org/10.1093/nar/28.1.27> PMID: 10592173
53. Marinho CM, Dos Santos PT, Kallipolitis BH, Johansson J, Ignatov D, Guerreiro DN, et al. The σ B-dependent regulatory sRNA Rli47 represses isoleucine biosynthesis in *Listeria monocytogenes* through a direct interaction with the *ilvA* transcript. *RNA Biol*. 2019; 16: 1424–1437. <https://doi.org/10.1080/15476286.2019.1632776> PMID: 31242083
54. Brenner M, Lobel L, Borovok I, Sigal N, Herskovits AA. Controlled branched-chain amino acids auxotrophy in *Listeria monocytogenes* allows isoleucine to serve as a host signal and virulence effector. *PLoS Genet*. 2018; 14: e1007283. <https://doi.org/10.1371/journal.pgen.1007283> PMID: 29529043
55. Dutta V, Elhanaf D, Kathariou S. Conservation and Distribution of the Benzalkonium Chloride Resistance Cassette bcrABC in *Listeria monocytogenes*. *Appl Environ Microbiol*. 2013; 79: 6067–6074. <https://doi.org/10.1128/AEM.01751-13> PMID: 23892748
56. Elhanafi D, Utta V, Kathariou S. Genetic characterization of plasmid-associated benzalkonium chloride resistance determinants in a *Listeria monocytogenes* strain from the 1998–1999 outbreak. *Appl Environ Microbiol*. 2010; 76: 8231–8238. <https://doi.org/10.1128/AEM.02056-10/ASSET/4E7916C1-4D47-44D6-997A-D8EC8CB7E6FC/ASSETS/GRAPHIC/ZAM9991016160005.JPEG>
57. Müller A, Rychli K, Muhterem-Uyar M, Zaiser A, Stessl B, Guinane CM, et al. Tn6188—A Novel Transposon in *Listeria monocytogenes* Responsible for Tolerance to Benzalkonium Chloride. *PLoS One*. 2013; 8: e76835. <https://doi.org/10.1371/journal.pone.0076835> PMID: 24098567

58. Chen GY, Kao CY, Smith HB, Rust DP, Powers ZM, Li AY, et al. Mutation of the Transcriptional Regulator Ytol Rescues *Listeria monocytogenes* Mutants Deficient in the Essential Shared Metabolite 1,4-Dihydroxy-2-Naphthoate (DHNA). *Infect Immun*. 2020;88. <https://doi.org/10.1128/IAI.00366-19> PMID: 31685546
59. Kelliher JL, Grunenwald CM, Abrahams RR, Daanen ME, Lew CI, Rose WE, et al. PASTA kinase-dependent control of peptidoglycan synthesis via ReoM is required for cell wall stress responses, cytosolic survival, and virulence in *Listeria monocytogenes*. *PLoS Pathog*. 2021; 17: e1009881. <https://doi.org/10.1371/journal.ppat.1009881> PMID: 34624065
60. Schulz LM, Dreier F, de Sousa Miranda LM, Rismondo J. Adaptation mechanisms of *Listeria monocytogenes* to quaternary ammonium compounds. *Microbiol Spectr*. 2023;11. <https://doi.org/10.1128/spectrum.01441-23> PMID: 37695041
61. Fox EM, Leonard N, Jordan K. Physiological and transcriptional characterization of persistent and non-persistent *Listeria monocytogenes* isolates. *Appl Environ Microbiol*. 2011; 77: 6559–6569. <https://doi.org/10.1128/AEM.05529-11> PMID: 21764947
62. To MS, Favrin S, Romanova N, Griffiths MW. Postadaptational resistance to benzalkonium chloride and subsequent physicochemical modifications of *Listeria monocytogenes*. *Appl Environ Microbiol*. 2002; 68: 5258–5264. <https://doi.org/10.1128/AEM.68.11.5258-5264.2002> PMID: 12406712
63. Martínez-Suárez J V., Ortiz S, López-Alonso V. Potential impact of the resistance to quaternary ammonium disinfectants on the persistence of *Listeria monocytogenes* in food processing environments. *Front Microbiol*. 2016; 7: 638. <https://doi.org/10.3389/fmicb.2016.00638> PMID: 27199964
64. Walsh JP, Bell RM. Diacylglycerol kinase from *Escherichia coli*. 1992. pp. 153–162. [https://doi.org/10.1016/0076-6879\(92\)09019-Y](https://doi.org/10.1016/0076-6879(92)09019-Y) PMID: 1323028
65. Park YK, Lee JY, Ko KS. Transcriptomic analysis of colistin-susceptible and colistin-resistant isolates identifies genes associated with colistin resistance in *Acinetobacter baumannii*. *Clinical Microbiology and Infection*. 2015; 21: 765.e1–765.e7. <https://doi.org/10.1016/j.cmi.2015.04.009> PMID: 25911992
66. Guinane CM, Cotter PD, Ross RP, Hill C. Contribution of penicillin-binding protein homologs to antibiotic resistance, cell morphology, and virulence of *Listeria monocytogenes* EGDe. *Antimicrob Agents Chemother*. 2006; 50: 2824–2828. <https://doi.org/10.1128/AAC.00167-06> PMID: 16870778
67. McKay SL, Portnoy DA. Ribosome hibernation facilitates tolerance of stationary-phase bacteria to aminoglycosides. *Antimicrob Agents Chemother*. 2015; 59: 6992–6999. <https://doi.org/10.1128/AAC.01532-15> PMID: 26324267
68. Kremer PHC, Lees JA, Koopmans MM, Ferwerda B, Arends AWM, Feller MM, et al. Benzalkonium tolerance genes and outcome in *Listeria monocytogenes* meningitis. *Clinical Microbiology and Infection*. 2017; 23: 265.e1–265.e7. <https://doi.org/10.1016/j.cmi.2016.12.008> PMID: 27998823
69. Bolten S, Harrant AS, Skeens J, Wiedmann M. Nonsynonymous Mutations in *fepR* Are Associated with Adaptation of *Listeria monocytogenes* and Other *Listeria* spp. to Low Concentrations of Benzalkonium Chloride but Do Not Increase Survival of *L. monocytogenes* and Other *Listeria* spp. after Exposure to Benzalkonium Chloride Concentrations Recommended for Use in Food Processing Environments. *Appl Environ Microbiol*. 2022;88. <https://doi.org/10.1128/aem.00486-22> PMID: 35587542
70. Hussein SH, Samir R, Aziz RK, Toama MA. Two putative MmpL homologs contribute to antimicrobial resistance and nephropathy of enterohemorrhagic *E. coli* O157:H7. *Gut Pathog*. 2019; 11: 1–13. <https://doi.org/10.1186/S13099-019-0296-7/TABLES/1>
71. Bowman JP, Hages E, Nilsson RE, Kocharunchitt C, Ross T. Investigation of the *Listeria monocytogenes* Scott A acid tolerance response and associated physiological and phenotypic features via whole proteome analysis. *J Proteome Res*. 2012; 11: 2409–2426. <https://doi.org/10.1021/pr201137c> PMID: 22372944
72. Reith J, Mayer C. Peptidoglycan turnover and recycling in Gram-Positive bacteria. *Appl Microbiol Biotechnol*. 2011; 92: 1–11. <https://doi.org/10.1007/s00253-011-3486-x> PMID: 21796380
73. Casey A, Fox EM, Schmitz-Esser S, Coffey A, McAuliffe O, Jordan K, et al. Transcriptome analysis of *Listeria monocytogenes* exposed to biocide stress reveals a multi-system response involving cell wall synthesis, sugar uptake, and motility. 2014. <https://doi.org/10.3389/fmicb.2014.00068> PMID: 24616718
74. Dalet K, Cenatiempo Y, Cossart P, Glaser P, Amend A, Baquero-Mochales F, et al. A σ^{54} -dependent PTS permease of the mannose family is responsible for sensitivity of *Listeria monocytogenes* to mesentericin Y105. *Microbiology (N Y)*. 2001; 147: 3263–3269. <https://doi.org/10.1099/00221287-147-12-3263/CITE/REFWORKS>
75. Xue J, Hunter I, Steinmetz T, Peters A, Ray B, Miller KW. Novel activator of mannose-specific phosphotransferase system permease expression in *Listeria innocua*, identified by screening for pediocin ACh resistance. *Appl Environ Microbiol*. 2005; 71: 1283–1290. <https://doi.org/10.1128/AEM.71.3.1283-1290.2005> PMID: 15746330

76. Geldart K, Kaznessis YN. Characterization of class IIa bacteriocin resistance in *Enterococcus faecium*. *Antimicrob Agents Chemother*. 2017;61. <https://doi.org/10.1128/AAC.02033-16> PMID: 28115354
77. Vadyvaloo V, Arous S, Gravesen A, Hécharde Y, Chauhan-Haubrock R, Hastings JW, et al. Cell-surface alterations in class IIa bacteriocin-resistant *Listeria monocytogenes* strains. *Microbiology (N Y)*. 2004; 150: 3025–3033. <https://doi.org/10.1099/mic.0.27059-0> PMID: 15347760
78. Personnic N, Bruck S, Nahori MA, Toledo-Arana A, Nikitas G, Lecuit M, et al. The Stress-Induced Virulence Protein InIH Controls Interleukin-6 Production during Murine Listeriosis. *Infect Immun*. 2010; 78: 1979. <https://doi.org/10.1128/IAI.01096-09> PMID: 20176794
79. Rouquette C, Ripio MT, Pellegrini E, Bolla JM, Tascon RI, Vázquez-Boland JA, et al. Identification of a ClpC ATPase required for stress tolerance and in vivo survival of *Listeria monocytogenes*. *Mol Microbiol*. 1996; 21: 977–987. <https://doi.org/10.1046/j.1365-2958.1996.641432.x> PMID: 8885268
80. Rouquette C, De Chastellier C, Nair S, Berche P. The ClpC ATPase of *Listeria monocytogenes* is a general stress protein required for virulence and promoting early bacterial escape from the phagosome of macrophages. *Mol Microbiol*. 1998; 27: 1235–1245. <https://doi.org/10.1046/j.1365-2958.1998.00775.x> PMID: 9570408
81. Mc Cay PH, Ocampo-Sosa AA, Fleming GTA. Effect of subinhibitory concentrations of benzalkonium chloride on the competitiveness of *Pseudomonas aeruginosa* grown in continuous culture. *Microbiology (Reading)*. 2010; 156: 30–38. <https://doi.org/10.1099/mic.0.029751-0> PMID: 19815578
82. Nordholt N, Kanaris O, Schmidt SBI, Schreiber F. Persistence against benzalkonium chloride promotes rapid evolution of tolerance during periodic disinfection. *Nat Commun*. 2021;12. <https://doi.org/10.1038/S41467-021-27019-8> PMID: 34815390
83. Tandukar M, Oh S, Tezel U, Konstantinidis KT, Pavlostathis SG. Long-term exposure to benzalkonium chloride disinfectants results in change of microbial community structure and increased antimicrobial resistance. *Environ Sci Technol*. 2013; 47: 9730–9738. <https://doi.org/10.1021/es401507k> PMID: 23924280